Towards UAV-Based Multi-Baseline Interferometry for Accurate Digital Elevation Model Generation

Victor Mustieles-Perez[*#], Julian Kanz[†], Christina Bonfert[†], Alexander Grathwohl[†], Lucas Leonardo Lamberti[*], Sumin Kim[*], Gerhard Krieger[*#], and Michelangelo Villano[*]

[*]*Microwaves and Radar Institute, German Aerospace Center (DLR), Wessling, Germany*

[#]*Institute of Electrical-Electronic-Communications Engineering, Friedrich-Alexander-Universität (FAU), Erlangen, Germany*

victor.mustieles@fau.de

[†]*Institute of Microwave Engineering, Ulm University, Ulm, Germany*

***Abstract*— Unmanned Aerial Vehicle (UAV)-based synthetic aperture radar (SAR) systems enable very accurate and cost-effective monitoring of local areas with unprecedentedly short revisit intervals. Unlike current spaceborne systems, UAV-based SAR systems are often characterized by a large fractional bandwidth, a short-range geometry and a broad range of incidence angles, due to the wide antenna beamwidth. This paper discusses how to exploit these characteristics to generate very accurate digital elevation models (DEMs) by combining multi-baseline SAR interferometry (InSAR) and stereo radargrammetry to achieve a more robust unwrapping of the interferometric phase. Based on the theoretical analyses and the specific characteristics of the UAV scenario, a multi-baseline InSAR experiment was planned and conducted. The DEM performance analysis and the simulations show that large baselines result in height accuracies in the sub-decimeter range, where geometric and volume decorrelation become the limiting factors. The demonstration of these concepts paves the way to height measurements with unprecedented accuracy and will also be of paramount importance for the design of future wideband, multi-baseline, or multifrequency spaceborne SAR missions.**

Keywords—Synthetic aperture radar (SAR), digital elevation model (DEM), UAVs, interferometry, radargrammetry.

I. Introduction

Synthetic aperture radar (SAR) is widely used in remote sensing for Earth observation. It exploits the radar movement to obtain high-resolution images and monitor Earth's surface on a global scale [1]. The use of unmanned aerial vehicles (UAVs) for small-scale remote sensing has gained interest, since UAV technology currently allows for increased payload capacity, improved positioning accuracy and flying stability, and cost reductions [2] [3]. Compared to traditional air- and spaceborne systems, UAV-based SAR systems are cost-effective, easy to deploy, offer a higher flexibility in operation and enable very accurate and frequent monitoring of local areas. Furthermore, the possible flight configurations and available bandwidths are generally less constrained [4]. These features make them ideal for studying local-scale dynamic processes using densely sampled time-series, e.g., harvest monitoring, or obtaining digital elevation models (DEMs) with unprecedented horizontal resolution and vertical accuracy. Furthermore, UAVs are very attractive for demonstrating new space-based concepts involving multiple platforms, multiple frequency bands or large bandwidths [5].

Across-track interferometric SAR (InSAR) is a well-established technique that exploits the phase difference, known as interferometric phase, between two complex SAR images of the same scene acquired from slightly different positions. The most common product obtained are the DEMs, which contain the topographic information of the scene [6] [7]. In repeat-pass InSAR, the two SAR images are acquired at different times in monostatic mode, whereas in single-pass InSAR they are acquired at the same time using two spatially separated antennas in bistatic mode. To avoid undesired changes within the imaged scene that may compromise the quality of the resulting DEM, single-pass InSAR is preferred, but the complexity of the system raises since synchronization between radars is usually needed.

On the one hand, the height accuracy of the DEM improves as the distance between the antennas, known as geometric baseline, increases. On the other hand, the height accuracy is also affected by the interferometric coherence, i.e., the complex cross-correlation between the two SAR images. The decorrelation due to the geometric baseline is a contribution which causes a coherence loss due to the fact that the scene is imaged from different incidence angles, increases with the separation between antennas, and poses an upper limit to the baseline. There are as well other decorrelation sources that affect the performance, such as the limited signal-to-noise ratio (SNR), the temporal decorrelation (in the case of repeat-pass InSAR), and the volume decorrelation [8]. The use of large geometric baselines to optimize the performance poses as well other constraints, e.g., the interferometric phase unwrapping and the coregistration of the two SAR images, increasing the complexity of the system. Multi-baseline InSAR, which is very suitable for UAV-based systems, aims at solving these restrictions.

This paper analyses the constraints that arise in the context of a multi-baseline InSAR system, provides an overview of the expected interferometric performance when large baselines are used together with absolute ranging approaches, and discusses the main aspects that arise in the DEM performance estimation and planning of a measurement campaign with UAVs in order to demonstrate the theoretical outcomes.

II. Motivation and Constraints of Large Baselines

In SAR interferometry, the topographic height is calculated from the interferometric phase. The scaling factor between them is the height of ambiguity, $h_{2\pi}$, i.e., the height variation corresponding to an interferometric phase variation of 2π. The interferometric phase is typically characterized by the standard deviation (std.), σ_φ, and the 90th percentile, $\varphi_{90\%}$. Thus, the height accuracy may be computed as [8]:

$$\Delta h = h_{2\pi} \cdot (\Delta\varphi / 2\pi), \tag{1}$$

where $\Delta\varphi$ can be either σ_φ or $\varphi_{90\%}$. The height of ambiguity decreases as the geometrical baseline increases, whereas the

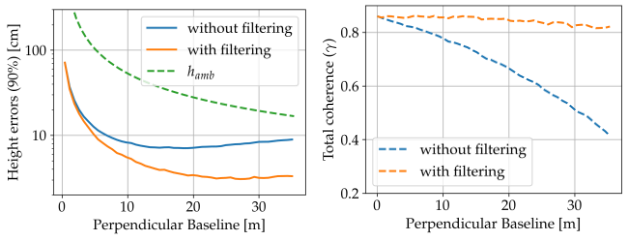

Fig. 1. Simulated height accuracy ($\Delta h_{90\%}$) and height of ambiguity with and without filtering the signals to a common frequency band (left) and total coherence (right) as a function of the perpendicular baseline.

accuracy of the interferometric phase worsens, mainly due to the effect of the geometric baseline decorrelation supposing all other decorrelation effects stay approximately constant. Therefore, depending on the mentioned contributions, there should be a baseline or an interval of baselines that optimize the performance. The height accuracy has been computed through a Monte Carlo simulation and plotted in the left-hand side of Fig. 1 as a function of the perpendicular baseline for a platform altitude, H, of 100 m, an incident angle, θ, of 45°, a bandwidth, B_{Rg}, of 3 GHz, and a central frequency, f_0, of 3 GHz. A reasonable coherence of 0.85 is assumed due to decorrelation sources other than the geometric baseline, and a post-spacing of 0.25 m in the final DEM is selected. The evolution of the total coherence is depicted in the right-hand side of Fig. 1. The achieved performance improves notably up to baselines of around 5 – 10 m, then it mostly stays stable for larger baselines. Narrowband spaceborne systems work in the region of very small baselines, thus underutilizing the system's full capability. Hence, attending to the obtained performance, a large baseline around 5 – 10 m (corresponding to approximately 10 – 15 % of the critical baseline) should be a good compromise between performance and complexity.

Making use of such large baselines implies as well some challenges. Firstly, coregistration complexity increases with the baseline, since larger baselines require a more accurate a priori height information for a given coregistration accuracy. A geometric coregistration is typically performed in first place as detailed in [9]. For a short-range geometry with large baselines, long-range approximations do not hold for the interferometric angle, $\Delta\theta$, i.e., the difference between the incident angles of both platforms, hence the accuracy in range dimension in units of pixels, Δi, may be expressed as:

$$|\Delta i| = \frac{\sin\Delta\theta}{\sin\theta_1 \Delta rg}|\Delta h|, \tag{2}$$

being Δh the height accuracy of the DEM used to coregister, and Δrg the resolution in range, assumed the same for both platforms, and where $\Delta\theta$ may be instead written as:

$$\Delta\theta = \arctan\left(\frac{B_\perp}{R - B_\parallel}\right), \tag{3}$$

with $B_\perp$ and $B_\parallel$ the perpendicular and parallel baselines, and R the slant range. Even if the coregistration is often refined afterwards using patch-wise cross-correlation, a very accurate result is needed to maximize the overlap between patches. This is even more important in a short-range geometry with dissimilar incident angles between radar platforms, which yields notable differences in ground range resolution and hence in the size of the patches if the SAR images are not properly coregistered. For an accuracy of 1/4 pixel, a baseline of 10 % of the critical baseline (the large baseline selected from Fig. 1), and $B_{Rg} = f_0 = 3\,GHz$, a DEM with a 0.5 m height accuracy is needed, which can be obtained from a second acquisition using a small baseline. Hence, as the small baseline shall be chosen considering the height accuracy required to coregister the SAR images acquired with the large baseline, a small baseline of 1 meter (approximately 2 % of the critical baseline) should be a good option.

III. Correction of Phase Unwrapping Errors

The classic phase unwrapping approach reaches its limit for the case of the large baselines that become usable with the broad bandwidth available in UAVs and in future spaceborne SAR missions. Multi-baseline InSAR benefits from the advantages of both small and large baselines. The former are used to obtain a less accurate DEM in which phase unwrapping errors are unlikely to occur due to the large height of ambiguity, while the latter are used to generate more accurate DEMs, whose unwrapping errors can be solved by combining the two generated DEMs with techniques that compare the phase gradients between the co-registered interferograms [10] or that resolve the height ambiguity independently for each pixel [11]. These multi-baseline techniques can be combined as well with absolute ranging approaches, e.g., stereo radargrammetry. Their use is, however, constrained by the bandwidth of the system, since in general it is needed that $\Delta h_{abs}/h_{2\pi} \ll 1$ to be able to correct phase unwrapping errors, being Δh_{abs} the height accuracy of radargrammetry [12]. If the same acquisition is used to perform the interferometric and radargrammetric processing, i.e., both have the same acquisition parameters, the ratio can be written as:

$$\frac{\Delta h_{abs}}{h_{amb}} = \frac{f_0}{B_{Rg}}\sigma_{\Delta x}, \tag{4}$$

where $\sigma_{\Delta x}$ is the achieved co-registration accuracy in terms of resolution cells. If coherent cross-correlation is used, $\sigma_{\Delta x}$ (Cramer-Rao bound of std.) is given by [13]:

$$\sigma_{\Delta x} = \sqrt{\frac{3}{2N}}\frac{\sqrt{1-\gamma^2}}{\pi\gamma} \tag{5}$$

where γ is the interferometric coherence and N is the used multi-looking, i.e. number of averaged cells.

The left-hand side of Fig. 2 presents an overview of the expected performance from stereo radargrammetry in comparison with interferometry for the same UAV system, considering a perpendicular baseline corresponding to 10% of the critical baseline, an incident angle of 45°, an interferometric coherence of 0.8, and a multi-looking factor of 12. It becomes clear how the expected performance of radargrammetry becomes comparable to the one expected from interferometry and that from fractional bandwidths of 0.1 it is already smaller than the interferometric height of ambiguity. The right-hand side of Fig. 2 shows the ratio $\Delta h_{abs}/h_{2\pi}$ as a function of the fractional bandwidth, specifying as well the location of several current and future spaceborne systems within the plot: TanDEM-X (9.85 GHz, 150 MHz), Tandem-L (1.27 GHz, 85 MHz) and HRWS (high-resolution wide-swath SAR, 9.85 GHz, 1.2 GHz). For TanDEM-X and Tandem-L, the ratio is large (5 and 2 respectively), thus phase unwrapping errors on the level of a single height of ambiguity cannot be detected. However, it becomes already smaller than 1 for HRWS (0.7), and even smaller for the UAVs (0.08). Even if the height accuracy of radargrammetry is given in terms of the Cramer Rao bound, Monte Carlo simulations have been performed as well. The shifts between the two SAR images were calculated in a two-

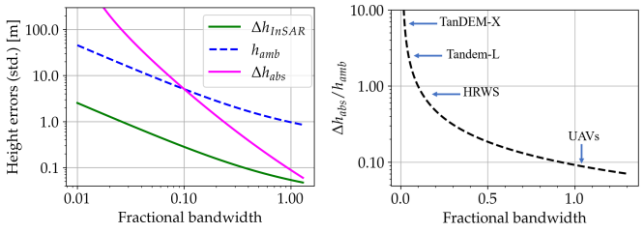

Fig. 2. Height accuracy predicted for interferometry and radargrammetry (left) and ratio $\Delta h_{abs}/h_{amb}$ (right).

step coregistration process. First, performing a coarse geometrical coregistration [9], then the result was refined using patch-wise coherent cross-correlation. Achieved height accuracies resulted to be in the order of 20 % worse than predicted from the Cramer Rao bound.

IV. Experimental Demonstration with UAVs

A measurement campaign for multi-baseline repeat-pass InSAR has been planned and performed in order to corroborate the theoretical and simulation outcomes in a real interferometric scenario. The demonstration of these results using UAVs will offer a very valuable information for the preparation of future wideband spaceborne missions. A broad and thorough DEM performance analysis has been conducted beforehand for each of the tested configurations. The analysis is based on the well-known spaceborne scenario [8], but special considerations are taken into account in order to model the specific features of the UAV system, e.g., wide bandwidth signals, short-range geometry, wide antenna beamwidth and worse flying and localization accuracy. Some of the most important points are discussed in the following.

The UAV-mounted radar system considered is detailed in [4] [14]. To compute the SNR, the system parameters from Table 1 and the sigma nought model for soil and rock, VV, L-band from [15] are assumed. The main contribution to volume decorrelation is considered to be ground penetration, which is computed for a mid-moisturized soil using the model in [16]. The geometric baseline decorrelation is modelled as presented in [17]. Range and azimuth ambiguities are negligible due to the low flying altitudes of the UAVs and the low speeds, respectively. Instead, right-left ambiguities are considered due to the wide antenna beamwidth. The geometric and volume decorrelations are the most important contributions and have a greater impact on the steepest incident angles and large baselines, in contrast to spaceborne systems, where the finite SNR is the limiting factor.

The predicted height accuracies of the DEM are in the sub-decimeter range for an independent post-spacing of 0.25 m × 0.25 m. Fig. 3 shows the predicted height accuracy for the aforementioned UAV system, a platform altitude of 20 m above ground level and different horizontal baselines. The height accuracy improves as the baselines increase. However, the height accuracy deteriorates for steep incident angles and very large baselines due to the effects of the geometric baseline and volume decorrelation. Furthermore, some additional degradation sources may have an impact on the final DEM performance. The DEM may have a systematic displacement and tilt below 2 cm and 2 cm/m, respectively, and height errors lower than 10 cm, which are reduced to less than 3 cm for large baselines due to the 1 cm accuracy of the positioning system, which is a GNSS receiver with real-time kinematic (RTK) capabilities [4]. These additional errors are

Table 1. System parameters assumed in the DEM performance analysis.

Parameter	Value	Parameter	Value
Frequency band	1 - 4 GHz	Drone speed	2 m/s
Transmit power	10 dBm	Duty cycle	0.8
Noise figure	5 dB	Antenna gain	6 dBi
Additional losses	3 dB	Antenna mounting	45˚
Pulse repetition frequency	1 kHz	Beamwidth in azimuth	50˚
Signal quantization	12 bits	Beamwidth in elevation	60˚

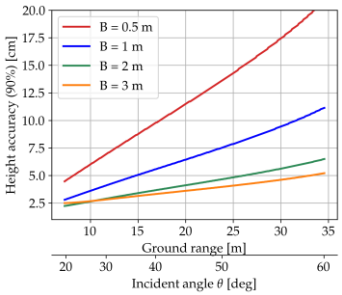

Fig. 3. Predicted height accuracy (90%) for a flying altitude of 20 m, different horizontal baselines, and an independent post-spacing of 0.25 m × 0.25 m.

reasonable but, however, are in the same order as the predicted height accuracy. An underestimation of them may therefore cause a severe degradation of the DEM.

V. Conclusion

Future wideband SAR systems offer the opportunity to use large interferometric baselines for the acquisition of high-resolution DEMs with unprecedented height accuracy. For the discussed UAV system, an interferometric baseline of around 10 % of the critical baseline was found to be a good compromise between performance and complexity, providing a spatial resolution of 25 cm and a height accuracy smaller than a decimeter. Challenges regarding phase unwrapping and coregistration will be solved by using multiple baselines and radargrammetry. Based on the analyses in this paper, a second and smaller baseline of around 2 % of the critical baseline should be a good choice.

A measurement campaign involving a large number of acquisitions in a variety of interferometric configurations has been carefully planned and successfully performed on June 1, 2023 to validate the theoretical predictions and simulations outlined in this paper. The results of these experiments will not only open the door to a new generation of DEMs for a variety of applications, but will also serve for the preparation of future wide-band, multi-frequency and/or multi-platform spaceborne SAR missions, such as HRWS.

Acknowledgment

This work was partially funded by the Deutsche Forschungsgemeinschaft (DFG, German Research Foundation) GRK 2680 – Project-ID 437847244. Co-funded by the European Union (ERC, DRITUCS, 101076275). Views and opinions expressed are however those of the authors only and do not necessarily reflect those of the European Union or the European Research Council Executive Agency. Neither the European Union nor the granting authority can be held responsible for them.

REFERENCES

[1] A. Moreira, P. Prats-Iraola, M. Younis, G. Krieger, I. Hajnsek, and K. P. Papathanassiou, “A tutorial on synthetic aperture radar,” IEEE Geosci. Remote Sens. Mag., vol. 1, no. 1, pp. 6–43, Mar. 2013.

[2] P. Hügler, F. Roos, M. Schartel, M. Geiger, and C. Waldschmidt, "Radar Taking Off: New Capabilities for UAVs," in IEEE Microwave Magazine, vol. 19, no. 7, pp. 43-53, Nov.-Dec. 2018.

[3] A. Grathwohl et al., "Taking a Look Beneath the Surface: Multicopter UAV-Based Ground-Penetrating Imaging Radars," in IEEE Microwave Magazine, vol. 23, no. 10, pp. 32-46, Oct. 2022.

[4] R. Bahnemann et al., “Under the sand: Navigation and localization of a micro aerial vehicle for landmine detection with ground-penetrating synthetic aperture radar,” Field Robotics, 2021.

[5] M. Villano *et al*., “Potential of Multi-Static SAR Systems for Earth Monitoring and Their Demonstration Using Swarms of Drones,” IGARSS 2023, Pasadena, CA, USA, 16-21 July 2023.

[6] R. Bamler and P. Hartl, “Synthetic aperture radar interferometry,” Inverse Problems, vol. 14, Art. no. 4, Aug. 1998.

[7] P. A. Rosen et al., “Synthetic aperture radar interferometry,” Proceedings of the IEEE, vol. 88, Art. no. 3, Mar. 2000.

[8] G. Krieger et al., “TanDEM-X: A Satellite Formation for High-Resolution SAR Interferometry,” IEEE Transactions on Geoscience and Remote Sensing, vol. 45, Art. no. 11, Nov. 2007.

[9] E. Sansosti, P. Berardino, M. Manunta, F. Serafino, and G. Fornaro, "Geometrical SAR image registration," IEEE Transactions on Geoscience and Remote Sensing, vol. 44, no. 10, pp. 2861-2870, Oct. 2006.

[10] A. Ferretti, A. Monti Guarnieri, C. Prati, F. Rocca, Multi Baseline Interferometric Techniques and Applications, in ESA Workshop on Applications of ERS SAR Interferometry 1996, Zurich, Switzerland.

[11] D. Massonnet, H. Vadon,, M. Rossi, Reduction of the Need for Phase Unwrapping in Radar Interferometry, IEEE Trans. Geosci. Remote Sens., Vol. 32, No. 2, pp.489-497, 1996.

[12] G. Krieger and A. Moreira, “Multistatic SAR satellite formations: potentials and challenges,” in Proceedings. 2005 IEEE International Geoscience and Remote Sensing Symposium, 2005. IGARSS ’05., 2005, vol. 4, pp. 2680–2684.

[13] R. Bamler and M. Eineder, "Split band interferometry versus absolute ranging with wideband SAR systems," IGARSS 2004. 2004 IEEE International Geoscience and Remote Sensing Symposium, Anchorage, AK, USA, 2004, pp. 980-984 vol.2.

[14] R. Burr et al., “UAV-Borne FMCW InSAR for Focusing Buried Objects,” in IEEE Geoscience and Remote Sensing Letters, vol. 19, pp. 1–5, 2022.

[15] F. Ulaby, M. Craig Dobson, and J. L. Alvarez Perez. Handbook of Radar Scattering Statistics for Terrain. Norwood, MA: Artech House, 1989

[16] M. T. Hallikainen, F. T. Ulaby, M. C. Dobson, M. A. El-rayes and L. -k. Wu, "Microwave Dielectric Behavior of Wet Soil-Part 1: Empirical Models and Experimental Observations," in IEEE Transactions on Geoscience and Remote Sensing, vol. GE-23, no. 1, pp. 25-34, Jan. 1985.

[17] V. Mustieles-Perez, S. Kim, C. Bonfert, G. Krieger, and M. Villano, “Towards UAV-Based Ultra-Wideband Multi-Baseline SAR Interferometry,” EuRAD 2023, Berlin, Germany, 20-22 September 2023.